

Dynamical Locking of the Chiral and the Deconfinement Phase Transition in QCD

Jens Braun and Alexander Janot

Theoretisch-Physikalisches Institut, Friedrich-Schiller-Universität Jena, D-07743 Jena, Germany

We study the fixed-point structure of four-fermion interactions in two-flavor QCD with N_c colors close to the finite-temperature phase boundary. In particular, we analyze how the fixed-point structure of four-fermion interactions is related to the confining dynamics in the gauge sector. We show that there exists indeed a mechanism which dynamically locks the chiral phase transition to the deconfinement phase transition. This mechanism allows us to determine a window for the values of physical observables in which the two phase transitions lie close to each other.

I. INTRODUCTION

The relation of quark confinement and chiral symmetry breaking in quantum chromodynamics (QCD) is not yet fully understood. In particular at finite temperature and quark chemical potential the investigation of the QCD phase boundary represents one of the major research topics in theoretical physics and is also of great importance for a better understanding of heavy-ion collision experiments [1]. Theoretical studies in the limit of many colors in fact suggest that an understanding of the interrelation of the chiral and the deconfinement phase transition is required to comprehend the QCD phase structure close to a possible critical endpoint [2].

While the confinement transition is driven by the gauge degrees of freedom, the chiral phase transition is triggered by strong quark self-interactions. In Nambu–Jona-Lasinio (NJL) models (and in the Polyakov-loop extended version thereof) these quark interactions are considered as parameters [3–14] and used to fit a given set of low-energy observables. In full QCD, however, we expect that the quark self-interactions are dynamically generated and driven to criticality by the gauge degrees of freedom. This has indeed been confirmed by means of a renormalization group (RG) analysis of the influence of gluodynamics on the fixed-point structure of four-fermion interactions, see e. g. Refs. [15–21]: once the gauge coupling exceeds a critical value, the quark sector is driven to criticality without requiring any fine-tuning. This observation already suggests that there might be a deeper relation between the chiral dynamics in the matter sector and the confining dynamics in the gauge sector and serves as a motivation for the present study.

The deconfinement phase transition has been studied in pure $SU(N_c)$ gauge theories and in QCD with lattice simulations, see e. g. Refs. [22–32], as well as functional continuum methods [33–40]. In so-called PNJL and Polyakov-loop extended quark-meson (QM) models a background field $\langle A_0 \rangle$ is introduced to study some aspects of quark confinement and the associated phase transition. This background field can be related to the so-called Polyakov variable $L[A_0]$,

$$L[A_0] = \frac{1}{N_c} \mathcal{P} \exp \left(i\bar{g} \int_0^\beta dx_0 A_0(x_0, \vec{x}) \right), \quad (1)$$

where β is the inverse temperature, N_c is the number of colors, \bar{g} denotes the bare gauge coupling and \mathcal{P} stands for path ordering. In fact, it has been shown that $\text{tr}_F L[\langle A_0 \rangle]$ serves as an order parameter for quark confinement in Polyakov-Landau-DeWitt gauge [33, 34] where $\langle A_0 \rangle$ is an element of the Cartan subalgebra and denotes the ground state of the associated order-parameter potential in the adjoint gauge algebra.¹ This potential can be computed, e. g., from the knowledge of gauge correlation functions. In Fig. 1 we show the results for the order-parameter potential as obtained from a first-principles RG study [33, 39]. The order parameter $\text{tr}_F L[\langle A_0 \rangle]$ is related to the standard Polyakov loop $\langle \text{tr}_F L[A_0] \rangle$ via the Jensen inequality,

$$\text{tr}_F L[\langle A_0 \rangle] \geq \langle \text{tr}_F L[A_0] \rangle. \quad (2)$$

In PNJL/PQM model studies one of the underlying approximations is to set $\text{tr}_F L[\langle A_0 \rangle] = \langle \text{tr}_F L[A_0] \rangle$. This opens up the possibility to incorporate results for the Polyakov loop $\langle \text{tr}_F L[A_0] \rangle$ as obtained from lattice simulations in these studies [3–14]. It is then found that the chiral and the deconfinement phase transition lie indeed close to each other at small values of the quark chemical potential, as one would naively expect it to be the case in full QCD [22–25, 27, 29–32]. However, the inclusion of the Polyakov loop in PNJL/PQM model studies by means of a Polyakov-loop potential is not unique and the QCD phase boundary at finite chemical potential has indeed been found to be very sensitive to different parameterizations of this potential, see e. g. Ref. [41]. On the other hand the data for the order parameter $L[\langle A_0 \rangle]$ is available. Therefore it seems natural to study at least some of the consequences of the approximation $\text{tr}_F L[\langle A_0 \rangle] = \langle \text{tr}_F L[A_0] \rangle$ underlying these model studies.

Recently, so-called dual observables arising from a variation of the boundary conditions of the fermions in time-like direction have been introduced [42] and employed for

¹ Strictly speaking, we have to distinguish between the background temporal gauge field in Landau-DeWitt gauge and its expectation value associated with the order parameter for confinement, see Refs. [33, 39]. We skip this subtlety here since it is of no importance for the present paper and refer to $\langle A_0 \rangle$ as the position of the ground-state of the order-parameter potential.

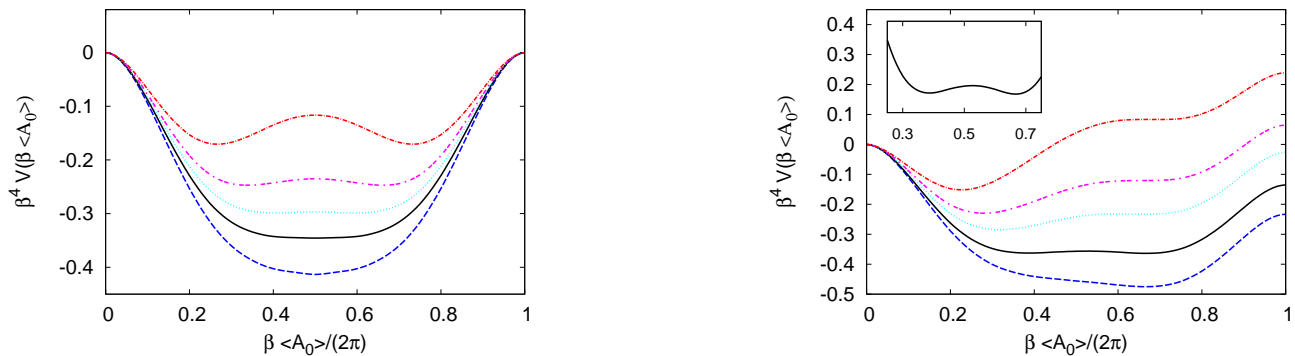


Figure 1: Normalized order-parameter potential $V(\beta\langle A_0 \rangle)$ for $SU(2)$ (left panel) and $SU(3)$ (right panel) Yang-Mills theories for various temperatures as obtained from a first-principles RG study [33]. For $SU(2)$ we show the potential for temperatures between $T = 260$ MeV and $T = 285$ MeV (from bottom to top). For $SU(3)$ the Cartan subalgebra is two-dimensional and, in turn, the potential depends on two independent variables. Here, we show only a slice of the potential for various temperatures between $T = 285$ MeV and $T = 310$ MeV (from bottom to top) in the relevant direction of the Cartan subalgebra. The first-order phase transition in $SU(3)$ Yang-Mills theory is indicated by a jump in the position of the minimum, see also the inlay of the figure. The phase transition temperature is $T_d \approx 266$ MeV for $SU(2)$ and $T_d \approx 290$ MeV for $SU(3)$, respectively.

a study of the relation of quark confinement and chiral symmetry breaking at finite temperature [35–38, 43–50]. These dual observables relate the spectrum of the Dirac operator to the order parameter for confinement, namely the Polyakov loop. The introduction of these observables constitutes an important formal advance which allows us to gain a deeper insight into the underlying dynamics at the QCD phase boundary. However, they do not allow us to fully resolve the question regarding the relation of quark confinement and chiral symmetry breaking.

In this work we aim to shed more light on the question under which circumstances the chiral and the deconfinement transition lie close to each other². To this end, we analyze the deformation of the RG fixed-point structure of chiral four-fermion interactions due to confining gauge dynamics in Sect. II. As detailed in Refs. [15–19, 51] these four-fermion interactions can then be easily connected to the QCD Lagrangian at high momentum scales. In Sect. III we then present our results for a partially bosonized formulation of the ansatz discussed in Sect. II. In particular, a necessary condition for an exact mapping of both the fermionic and the partially bosonized theory is discussed. As one of our main results, we present a phase diagram spanned by the temperature and the pion decay constant f_π . The latter is directly related to the chiral condensate. This phase diagram allows us to gain some insight into the interrelation of quark confinement and chiral symmetry breaking. In contrast to the phenomenologically more relevant phase diagram spanned by the temperature and quark chemical potential, the

(T, f_π) phase diagram can be studied by various different approaches without suffering from problems, e. g., arising from a complex-valued Dirac operator. A study of the (T, f_π) phase diagram may therefore be helpful to, e. g., benchmark continuum approaches with the aid of lattice simulations. Our concluding remarks and possible future extensions of the present study are given in Sect. IV.

II. FERMIONIC FIXED-POINT STRUCTURE AND THE LOCKING MECHANISM

We start our discussion of a dynamical locking mechanism for the chiral phase transition with an analysis of the fixed-point structure in the matter sector of QCD. For our study we employ an RG equation for the quantum effective action, the Wetterich equation [52]. The effective action Γ then depends on the RG scale k (infrared cutoff scale) which determines the RG ‘time’ $t = \ln(k/\Lambda)$ with Λ being a UV cutoff scale. For reviews on and introductions to this functional RG approach we refer the reader to Refs. [53–61].

For our more general discussion in this section, it suffices to consider the following ansatz for the effective action:

$$\Gamma_k[\bar{\psi}, \psi, \langle A_0 \rangle] = \int d^4x \left\{ Z_\psi \bar{\psi} (i\not{\partial} + \bar{g}\gamma_0 \langle A_0 \rangle) \psi + \frac{\bar{\lambda}_\psi}{2} [(\bar{\psi}\psi)^2 - (\bar{\psi}\vec{\tau}\gamma_5\psi)^2] \right\}, \quad (3)$$

For $\bar{\lambda}_\psi \equiv 0$ this ansatz can be considered as the microscopic matter part of the QCD action functional in Landau-DeWitt gauge. In the present work we restrict ourselves to $N_f = 2$ massless quark flavors and N_c colors. The τ_i ’s represent the Pauli matrices and couple

² In full QCD with light but finite quark masses both transitions are crossovers. Since there is no unique way to define the critical temperature associated with a crossover, a proof of an exact coincidence of the two transitions seems to be impossible in any case.

the spinors in flavor space. The coupling $\bar{\lambda}_\psi$ is considered to be RG-scale dependent. Note that fermionic self-interactions are fluctuation-induced in full QCD, e. g. by two-gluon exchange, and are therefore not fundamental, see Refs. [15–20] for a detailed discussion.

Our ansatz for the effective action can be considered as the leading order in a systematic derivative expansion of the fermionic sector of QCD. The associated small parameter of such an expansion is the anomalous dimension $\eta_\psi = -\partial_t \ln Z_\psi$ of the fermion fields which has indeed been found to be small in earlier studies with vanishing background field $\langle A_0 \rangle$, see Refs. [15, 19, 62, 63]. In the following we therefore set the wave-function renormalization $Z_\psi \equiv 1$.

In this section we also drop a possible momentum dependence of the four-fermion coupling, $\lambda_\psi(|p| \ll k)$. This approximation does not permit a study of properties, such as the meson mass spectrum, in the chirally broken regime; for example, mesons manifest themselves as momentum singularities in the four-fermion couplings. However, the point-like limit can still be a reasonable approximation in the chirally symmetric regime above the chiral phase transition which allows us to gain some insight into the question how the theory approaches the regime with broken chiral symmetry in the ground state [17–19]. For our more quantitative analysis in Sect. III we shall partly resolve the momentum dependence of the fermionic interactions in order to gain access to low-energy observables. At this point it is important to stress that in the point-like limit the RG flow of the four-fermion coupling, which signals the onset of chiral symmetry breaking, is completely decoupled from the RG flow of fermionic n -point functions of higher order. For example, 8-fermion interactions do not contribute to the RG flow of the coupling $\bar{\lambda}_\psi$ in this limit.

The constant background field $\langle A_0 \rangle$ in our ansatz (3) is an element of the Cartan subalgebra and can be parametrized in terms of the corresponding generators

$$\begin{aligned} \beta \bar{g} \langle A_0 \rangle &= 2\pi \sum_{T^a \in \text{Cartan}} T^a \phi^{(a)} \\ &= 2\pi \sum_{T^a \in \text{Cartan}} T^a v^{(a)} |\phi|, \quad v^2 = 1, \end{aligned} \quad (4)$$

where the T_a 's denote the generators of the underlying $SU(N_c)$ gauge group in the fundamental representation³. It is convenient to introduce the eigenvalues ν_l of the hermitian matrix in Eq. (4):

$$\nu_l = \text{spec} \{ (T^a v^a)_{ij} \mid v^2 = 1 \}. \quad (5)$$

The presence of a finite background field $\langle A_0 \rangle$ now yields a fermion propagator $(\Gamma^{(2)})^{-1}$ (inverse two-point function) which is no longer proportional to the identity $\mathbb{1}$ in

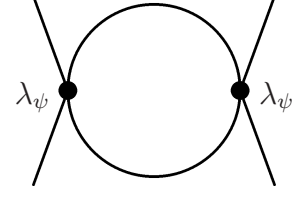


Figure 2: Representation of the 1PI Feynman diagram associated with the λ_ψ^2 -term on the right-hand side of the RG flow equation (7). Our functional RG study includes resummations of this diagram to arbitrary order in λ_ψ .

color space. However, it can be spanned by the Cartan subalgebra as follows:

$$\begin{aligned} \left(\Gamma^{(2)}[\{\nu_l|\phi|\}] \right)_{ij}^{-1} &= \frac{1}{N_c} \left(\Gamma_0^{(2)}[\{\nu_l|\phi|\}] \right)^{-1} \mathbb{1}_{ij} \\ &+ \sum_{T^a \in \text{Cartan}} \left(\Gamma_a^{(2)}[\{\nu_l|\phi|\}] \right)^{-1} T_{ij}^a, \end{aligned} \quad (6)$$

Here, the T_{ij}^a 's denote the generators in the fundamental representation. The expansion coefficients on the right-hand side of Eq. (6) can be obtained straightforwardly by using $\text{tr}_F T^a T^b = \frac{1}{2} \delta_{ab}$ and $\text{tr}_F T^a = 0$. Of course, it is expected from a physical point of view that the expansion (6) of the fermion propagator is convenient once a background field $\langle A_0 \rangle$ is introduced into the theory since the latter distinguishes a direction in color space. For $\langle A_0 \rangle \equiv 0$ we have $(\Gamma_a^{(2)})^{-1} \equiv 0$.

Using the ansatz (3) together with the parametrization (6), we obtain the RG flow equation for the dimensionless renormalized four-fermion coupling λ_ψ in the point-like limit:

$$\begin{aligned} \beta_{\lambda_\psi} \equiv \partial_t \lambda_\psi &= (2 + 2\eta_\psi) \lambda_\psi \\ &- \frac{2}{\pi^2} \left(2 + \frac{1}{N_c} \right) \sum_{l=1}^{N_c} l_1^{(F)}(\tau, 0, \nu_l |\phi|) \lambda_\psi^2, \end{aligned} \quad (7)$$

where

$$\lambda_\psi = Z_\psi^{-2} k^2 \bar{\lambda}_\psi. \quad (8)$$

Note that λ_ψ depends on the background field $\langle A_0 \rangle$ and the dimensionless temperature $\tau = T/k$. The so-called threshold function $l_1^{(F)}$ corresponds to a one-particle irreducible (1PI) Feynman diagram, see Fig. 2, and describes the decoupling of massive and thermal modes. Moreover, the regularization scheme dependence is encoded in these functions. The definition of the threshold function $l_1^{(F)}$ can be found in App. A.

Let us now discuss the fixed-point structure of the coupling λ_ψ . Apart from a Gaussian fixed point we have a second non-trivial fixed point. The value of this fixed point depends on the dimensionless temperature τ and the dimensionless coordinates $\{\nu_l|\phi|\}$ of the background

³ The dimension of the Cartan subalgebra is $N_c - 1$.

field $\langle A_0 \rangle$, see Fig. 3. At vanishing temperature (and background field $\langle A_0 \rangle$) we find

$$\begin{aligned} \lambda_\psi^* &= \frac{\pi^2}{(2N_c + 1)l_1^F(0, 0, 0)} + \mathcal{O}(\eta_\psi^*) \\ &= \frac{6\pi^2}{(2N_c + 1)} + \mathcal{O}(\eta_\psi^*) \end{aligned} \quad (9)$$

for the non-Gaussian fixed point. For illustration we have evaluated the threshold function $l_1^{(F)}$ in the second line for the regulator function (A2). Here, η_ψ^* denotes the value of the fermionic anomalous dimension at the fixed point. Note that the rescaled fixed-point coupling $N_c \lambda_\psi^*$ approaches a constant value in the limit $N_c \rightarrow \infty$.

The fixed-point value λ_ψ^* is not a universal quantity as its dependence on the threshold function indicates. However, the statement about the existence of the fixed point is universal. Choosing an initial value $\lambda_\psi^{\text{UV}} < \lambda_\psi^*$ at the initial UV scale Λ we find that the theory becomes non-interacting in the infrared regime ($\lambda_\psi \rightarrow 0$ for $k \rightarrow 0$), see Fig. 3. For $\lambda_\psi^{\text{UV}} > \lambda_\psi^*$ we find that the four-fermion coupling λ_ψ increases rapidly and diverges eventually at a finite scale k_{cr} . This behavior indicates the onset of chiral symmetry breaking associated with the formation of a quark condensate. Hence chiral symmetry breaking in the IR only occurs if we choose $\lambda_\psi^{\text{UV}} > \lambda_\psi^*$. Of course, the divergence of the four-fermion coupling at a finite scale k_{cr} is an artifact of our point-like approximation. It can be resolved by taking into account (some of) the momentum dependence of the coupling λ_ψ , see Sect. III. This will then allow us to gain access to QCD low-energy observables. In any case, the scale k_{cr} at which $1/\lambda_\psi(k_{\text{cr}}) = 0$ sets the scale for a given IR observable \mathcal{O} :

$$\mathcal{O} \sim k_{\text{cr}}^{d_{\mathcal{O}}} , \quad (10)$$

where $d_{\mathcal{O}}$ is the canonical mass dimension of the observable \mathcal{O} . At vanishing temperature the scale k_{cr} can be computed analytically. We find

$$k_{\text{cr}} = \Lambda \theta(\lambda_\psi^{\text{UV}} - \lambda_\psi^*) \left(\frac{\lambda_\psi^{\text{UV}} - \lambda_\psi^*}{\lambda_\psi^{\text{UV}}} \right)^{\frac{1}{2}} + \mathcal{O}(\eta_\psi^*) . \quad (11)$$

Thus, the critical value k_{cr} scales with the distance of the initial value λ_ψ^{UV} from the fixed-point value λ_ψ^* . For increasing λ_ψ^{UV} the scale k_{cr} increases and, in turn, the values of low-energy observables, such as the pion decay constant f_π and the chiral phase transition temperature T_χ , increase.

From now on, we assume that we fix $\lambda_\psi^{\text{UV}} > \lambda_\psi^*$ at $T = 0$. The value of λ_ψ^{UV} then determines the scale $k_{\text{cr}} \equiv k_{\text{cr}}(\lambda_\psi^{\text{UV}})$ which is related to the values of the low-energy values. For a study of the effects of a finite temperature and a finite background field $\langle A_0 \rangle$ we then leave our choice for λ_ψ^{UV} unchanged. This ensures comparability of the results at zero and finite temperature for a given theory defined by the choice for λ_ψ^{UV} at zero temperature.

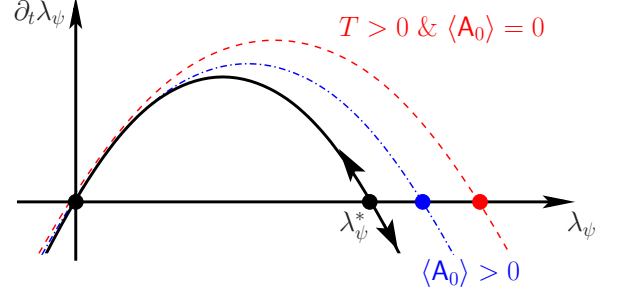


Figure 3: Sketch of the β function of the four-fermion interaction for three different cases: vanishing temperature (black/solid line), a given finite value of the temperature T and $\langle A_0 \rangle = 0$ (red/dashed line), the same temperature T but $\langle A_0 \rangle > 0$ (blue/dashed-dotted line). The arrows indicate the direction of the RG flow towards the infrared.

Next, we turn to a discussion of the fixed-point structure at finite temperature but vanishing background field $\langle A_0 \rangle$. We still have a Gaussian fixed point. Moreover, we find a pseudo fixed-point $\lambda_\psi^*(\tau)$ for arbitrary values of τ at which the right-hand side of the flow equation is zero:

$$\lambda_\psi^*(\tau) = \frac{\pi^2}{(2N_c + 1)l_1^{(F)}(\tau, 0, 0)} + \mathcal{O}(\eta_\psi^*) . \quad (12)$$

For high temperatures $T \gg k$ we find $\lambda_\psi^* \sim (T/k)^3$. Let us now assume that we have chosen $\lambda_\psi^{\text{UV}} > \lambda_\psi^*(\tau = 0)$. Since the value of the (pseudo) fixed-point increases with increasing T/k , the rapid increase of the four-fermion coupling towards the IR ($k \rightarrow 0$) is effectively slowed down and may even change its direction on the plane defined by the two-dimensional β_{λ_ψ} function⁴, see also Fig. 3. This behavior of the pseudo fixed-point $\lambda_\psi^*(\tau)$ already suggests that for a fixed initial value λ_ψ^{UV} a critical temperature T_χ exists above which the four-fermion coupling does not diverge but approaches zero in the IR. Such a behavior is indeed expected for high temperatures since the quarks become effectively stiff degrees of freedom due to their thermal mass $\sim T$ and chiral symmetry is restored.

Let us now turn to a discussion of the fixed-point structure for finite T and $\langle A_0 \rangle$. In the present approach we consider the value of the background field $\langle A_0 \rangle$ as an external input which is determined by the ground state of the corresponding order-parameter potential, see also Fig. 1. As discussed above, the position $\langle A_0 \rangle$ of the ground-state is directly related to our order parameter for confinement, $\text{tr}_F L[\langle A_0 \rangle]$. For temperatures much larger than the deconfinement phase-transition temperature T_d we have $\langle A_0 \rangle = 0$, i. e. $\text{tr}_F L[\langle A_0 \rangle] = 1$. On the other

⁴ At finite temperature the β_{λ_ψ} function depends on two variables, namely $\tau = T/k$ and λ_ψ .

hand, the position $\langle A_0 \rangle$ of the ground state in the confined phase of pure $SU(N_c)$ Yang-Mills theory is uniquely determined up to center transformations by [33, 39]

$$\text{tr}_F(L[\langle A_0 \rangle])^n = 0 \quad (13)$$

with $(n \bmod N_c) = 1, \dots, N_c - 1$. These conditions determine the $N_c - 1$ coordinates $\{\phi^{(a)}\}$ of $\langle A_0 \rangle$, see Eq. (4). Moreover, we have

$$\frac{1}{N_c} |\text{tr}_F(L[\langle A_0 \rangle])^n| \leq \frac{1}{N_c^n}. \quad (14)$$

$$\begin{aligned} \lambda_\psi^*(\tau, \langle A_0 \rangle) &= \left(\frac{1}{\pi^2} \left(2 + \frac{1}{N_c} \right) \sum_{l=1}^{N_c} l_1^{(F)}(\tau, 0, \nu_l|\phi|) \right)^{-1} \\ &= \left(\frac{1}{\lambda_\psi^*(0, 0)} + \frac{1}{6\pi^2} \left(2 + \frac{1}{N_c} \right) \sum_{n=1}^{\infty} (-N_c)^n [\text{tr}_F(L[\langle A_0 \rangle])^n + \text{tr}_F(L^\dagger[\langle A_0 \rangle])^n] \left(1 + \frac{n}{\tau} \right) e^{-\frac{n}{\tau}} \right)^{-1}, \end{aligned} \quad (15)$$

where we have dropped terms depending on η_ψ^* on the right-hand side. To obtain the second line we have employed the regulator function (A2). However, the general form of the asymptotic series (15) holds for any regulator function as can be shown by means of Poisson resummation techniques⁵. Note that the series (15) can be considered as an expansion for small $\tau = T/k$.

Using Eq. (13) we observe that all finite-temperature corrections to the fixed-point value vanish identically in the confined phase for $N_c \rightarrow \infty$, provided that the ground-state value $\langle A_0 \rangle$ is identical in $SU(N_c)$ Yang-Mills theory and QCD with dynamical fermions. Of course, the latter assumption is not exactly fulfilled but for physical quark masses it is reasonable to assume

$$\text{tr}_F L[\langle A_0 \rangle] \ll 1 \quad (16)$$

at low and intermediate temperatures. Thus, we have found that

$$\lambda_\psi^*(0, 0) \equiv \lambda_\psi^*(\tau, \langle A_0 \rangle) \quad (17)$$

in the limit $N_c \rightarrow \infty$, independent of the temperature T for $T \lesssim T_d$. On the other hand, we have

$$\lambda_\psi^*(\tau, \langle A_0 \rangle) \rightarrow \lambda_\psi^*(\tau, 0) \quad \text{for} \quad \langle A_0 \rangle \rightarrow 0. \quad (18)$$

With the same reasoning we find

$$\beta_{\lambda_\psi}(0, 0) \equiv \beta_{\lambda_\psi}(\tau, \langle A_0 \rangle) \quad (19)$$

for $T \lesssim T_d$ and $N_c \rightarrow \infty$. This means that for $T < T_d$ the question of whether chiral symmetry is spontaneously

broken or not is in fact *independent* of the temperature, but depends only on the choice of the initial value λ_ψ^{UV} relative to its fixed-point value λ_ψ^* at $T = 0$ and $\langle A_0 \rangle = 0$. We emphasize that Eqs. (17)-(19) are regularization-scheme independent statements. For any admissible so-called $3d$ regulator function, e. g. Eq. (A2), it is also possible to show analytically that

$$\lambda_\psi^*(0, 0) \leq \lambda_\psi^*(\tau, \langle A_0 \rangle) \leq \lambda_\psi^*(\tau, 0) \quad (20)$$

for arbitrary temperatures $\tau = T/k$ for $N_c = 2, 3$; see also discussion of Eq. (A10) in App. A. In any case, $\lambda_\psi^*(\tau, \langle A_0 \rangle)$ interpolates continuously for a given finite value of τ between $\lambda_\psi^*(0, 0)$ and $\lambda_\psi^*(\tau, 0)$.

Provided that we choose an initial value $\lambda_\psi^{\text{UV}} > \lambda_\psi^*(0, 0)$, it follows immediately from Eq. (19) that

$$T_\chi \geq T_d \quad (21)$$

for $N_c \rightarrow \infty$, see also Ref. [3]. This means that the chiral phase transition is locked in due to the confining dynamics in the gauge sector. Loosely speaking, thermal fluctuations of the quark fields, which tend to restore chiral symmetry, are suppressed since they are directly linked to the deconfinement order parameter. Thus, we have found that the restoration of chiral symmetry is intimately connected to the confining dynamics in the gauge sector.

In the present analysis the actual chiral phase transition temperature depends on two parameters, namely the value of the background field $\langle A_0 \rangle$ and the initial condition λ_ψ^{UV} . However, Eq. (21) is a parameter-free statement. It simply follows from an analysis of the effect of gauge dynamics on the fixed-point structure in the fermionic sector. In particular, we have only made use of

⁵ The sum over the τ -dependent terms in the second line of Eq. (15) is also closely related to the geometric series.

general properties of the deconfinement order parameter and the fact that $\lambda_\psi^{\text{UV}} > \lambda_\psi^*(0, 0)$ is a necessary condition for chiral symmetry breaking at $T = 0$ and $\langle A_0 \rangle = 0$. Of course, the initial condition λ_ψ^{UV} is not a free parameter in QCD but originally generated by quark-gluon interactions at high (momentum) scales. In a given regularization scheme the value of λ_ψ^{UV} can therefore in principle be related to the value of the strong coupling α_s at, e. g., the τ mass scale [16–19]. We would like to point out that neither the value of α_s at some scale nor the value of λ_ψ^{UV} on a given RG trajectory is a physical observable. However, their values can be related to physical low-energy observables. Recall that the value of λ_ψ^{UV} determines the critical scale k_{cr} which sets the scale for IR observables, see Eq. (11).

Our findings in the limit $N_c \rightarrow \infty$ even allow us to estimate a window in parameter space in which the chiral phase transition and the deconfinement phase transition lie close to each other. In our discussion of chiral symmetry breaking for vanishing background field $\langle A_0 \rangle$ we have argued that $T_\chi \sim k_{\text{cr}}$, where the scale k_{cr} is eventually determined by our choice for λ_ψ^{UV} . If we take into account the background field $\langle A_0 \rangle$, then the chiral phase transition temperature T_χ is locked in and we necessarily have $T_\chi \geq T_d$ in the large- N_c limit, see Eq. (21). Thus, the chiral phase transition temperature for all theories which would allow for $T_\chi \leq T_d$ for $\langle A_0 \rangle = 0$ is shifted such that $T_\chi \simeq T_d$. The upper end of the locking window can therefore be estimated by the smallest value for λ_ψ^{UV} for which T_χ for vanishing $\langle A_0 \rangle$ is still larger than T_d . Whereas λ_ψ^* and λ_ψ^{UV} are scheme-dependent quantities, the mere existence of such a window in parameter space is a universal statement. As we have argued above, the value λ_ψ^{UV} can be related to the values of physical low-energy observables. Therefore the existence of such a window for the initial condition λ_ψ^{UV} suggests the existence of a corresponding window for the values of low-energy observables. We shall come back to this below when we discuss the phase diagram in the plane spanned by the temperature and the pion decay constant.

Let us now discuss the relation of quark confinement and chiral symmetry breaking for finite N_c . In this case, terms with

$$n \bmod N_c = 0 \quad (22)$$

contribute to the right-hand side of Eq. (15) and to the RG flow of λ_ψ . We then find that the inequality (20) holds only for $\tau = T/k \ll 1$ but not for arbitrary values of τ . However, this does not necessarily imply that we do not have a finite range of values for the initial condition λ_ψ^{UV} anymore in which the chiral and the deconfinement phase transition are tightly linked. It only implies that the lower end of the window for λ_ψ^{UV} is shifted to larger values compared to the large- N_c limit.

To illustrate our analytic findings we have studied numerically the RG flow of the four-fermion coupling λ_ψ for finite N_c . In our setup, the phase transition temperature is defined to be the smallest temperature for which λ_ψ

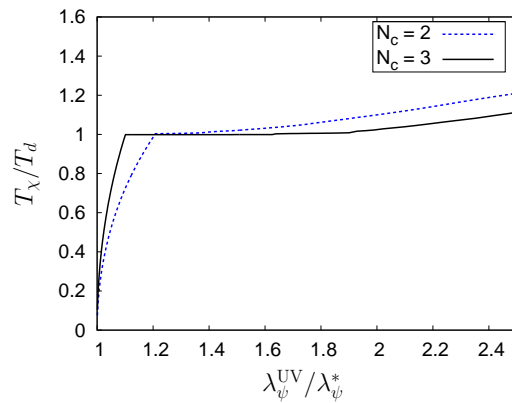


Figure 4: Phase diagram for two massless quark flavors and $N_c = 2$ colors (blue/dashed line) as well as for $N_c = 3$ colors (black/solid line) in the plane spanned by the temperature and the rescaled coupling $\lambda_\psi^{\text{UV}}/\lambda_\psi^*$. The lines depict our results for the ratio T_χ/T_d of the chiral and the deconfinement phase transition temperature as a function of $\lambda_\psi^{\text{UV}}/\lambda_\psi^*$. Recall that there is no splitting of the phase boundary (i. e. $T_\chi \simeq T_d$) for small λ_ψ^{UV} in the limit $N_c \rightarrow \infty$.

remains finite in the infrared limit $k \rightarrow 0$. Strictly speaking, this only yields an upper bound for the phase transition temperature since it is only sensitive to an emergence of a condensate on intermediate momentum scales but insensitive to a fate of the condensate in the deep IR due to fluctuations of the Goldstone modes [63]. In Fig. 4 we present the phase diagram for two massless quark flavors and $N_c = 2$ as well as $N_c = 3$ in the plane spanned by the temperature and the UV coupling λ_ψ^{UV} . To estimate the phase boundary we have employed the results for $\langle A_0 \rangle$ for the corresponding $SU(N_c)$ Yang-Mills theory as obtained in Refs. [33, 39], see also Fig. 1. The associated deconfinement phase transition temperature is $T_d \approx 266$ MeV for pure gauge $SU(2)$ and $T_d \approx 290$ MeV for pure gauge $SU(3)$, respectively. For the UV cutoff we have chosen $\Lambda = 1$ GeV. In accordance with our analytic findings we observe that there is only a chirally symmetric phase for $\lambda_\psi^{\text{UV}} < \lambda_\psi^*$. Taking into account corrections beyond the large- N_c approximation, we find that the chiral phase transition temperature increases continuously with λ_ψ^{UV} , $T_\chi \sim (\lambda_\psi^{\text{UV}} - \lambda_\psi^*)^{1/2}$, starting from $T_\chi = 0$ for $\lambda_\psi^{\text{UV}} = \lambda_\psi^*$. In this regime we have $T_d > T_\chi$. Increasing λ_ψ^{UV} further we find a window for the values of λ_ψ^{UV} in which we have $T_\chi \sim T_d$. In this regime the chiral phase transition is locked in due to the confining dynamics in the gauge sector. Note that T_χ is a strictly monotonously increasing function in λ_ψ^{UV} for $\langle A_0 \rangle = 0$. In agreement with our analytic results we observe that the size of this locking window increases with increasing N_c . For $\lambda_\psi^{\text{UV}} \gg \lambda_\psi^*$ we then observe that the phase transition temperatures T_d and T_χ differ again. However, we now have $T_\chi > T_d$.

At this point a few comments are in order. First, it is clear that the potential of the confinement order parameter in full QCD (and hence the position of the ground-

state $\langle A_0 \rangle$) also receives contributions from Feynman diagrams with at least one internal fermion line. These contributions tend to lower the deconfinement phase transition temperature⁶. We stress that we only use the Yang-Mills approximation for $\langle A_0 \rangle$ here to explore the impact of the discussed locking mechanism for the chiral phase transition on the finite-temperature phase structure. In any case, our analytic findings are not (strongly) affected by this approximation since they rely on very general properties of the confinement order parameter. Therefore we still expect that a window in parameter space exists in which the chiral and the deconfinement phase transition lie close to each other. However, our estimate of the phase diagram in the $(T, \lambda_{\psi}^{\text{UV}})$ -plane and the size of the locking window will change quantitatively when we take into account the corrections to $\langle A_0 \rangle$ due to quark fluctuations. In particular, we expect that below the locking window the difference T_{χ} and T_d becomes smaller since this regime is associated with quarks with a small dynamical mass. Second, our ansatz (3) for the effective action is not complete with respect to Fierz transformations, see e. g. Refs. [16–18, 64]; for example, we have dropped the so-called vector-channel interaction $\sim (\bar{\psi}\gamma_{\mu}\psi)^2$. Such interactions would also contribute to the RG flow of the four-fermion interaction λ_{ψ} . At finite temperature the minimal basis of point-like four-fermion interactions is larger than at vanishing temperature since the Poincare invariance is broken by the heat bath. If we allow for a finite $\langle A_0 \rangle$, the minimal set of point-like four-fermion interactions is even larger than in the case of vanishing background field $\langle A_0 \rangle$. This is due to the fact that a finite background field $\langle A_0 \rangle$ distinguishes a direction in color space. For example, our expansion (6) of the fermion propagator suggests that a finite background field $\langle A_0 \rangle$ gives rise to additional point-like interactions of the type $\sim (\bar{\psi}T^{(3)}\psi)^2$ and $\sim (\bar{\psi}T^{(8)}\psi)^2$ for $N_c = 3$. However, the additional diagrams are of the same topology as the one shown in Fig. 2. We therefore expect that the inclusion of additional four-fermion interactions associated with a Fierz-complete basis is particularly important for a quantitative computation of the chiral phase transition temperature beyond the large- N_c limit. Such an analysis is beyond the scope of this work and deferred to future studies.

Finally we would like to briefly comment on PNJL/PQM-type model studies which are closely related to the present study. In contrast to the present work, the PNJL/PQM-type model studies use the assumptions $\text{tr}_F L[\langle A_0 \rangle] = \langle \text{tr}_F L[A_0] \rangle$ and $N_c^n \text{tr}_F (L[\langle A_0 \rangle])^n = N_c \langle \text{tr}_F L[A_0] \rangle^n$, see e. g. Ref. [3]. If we used these assumptions, we would not have observed the regime with $T_{\chi} < T_d$ for small values of $(\lambda_{\psi}^{\text{UV}} - \lambda_{\psi}^*)$ and finite N_c where the two phase transitions are decoupled. As we have dis-

cussed above, the decoupling of the phase transitions for small values of $(\lambda_{\psi}^{\text{UV}} - \lambda_{\psi}^*)$ is only absent in the limit $N_c \rightarrow \infty$ in our study. Therefore we conclude that these approximations used in PNJL/PQM-type model studies correspond to a large- N_c approximation in the coupling of the matter and the gauge sector. This type of large- N_c approximation should not be confused with the large- N_c approximations used in the matter sector of these models, such as neglecting pion fluctuations. In any case, our analysis shows that the large- N_c approximation associated with the approximation $\text{tr}_F L[\langle A_0 \rangle] = \langle \text{tr}_F L[A_0] \rangle$ clearly affects the dynamics near the finite-temperature phase boundary and may therefore also affect the predictions for the (T, μ) phase diagram from PNJL/PQM-type models.

III. THE LOCKING MECHANISM AND THE (T, f_{π}) PHASE DIAGRAM

In the previous section we have discussed the interrelation of quark confinement and chiral symmetry breaking in a purely fermionic language. We have found that there exists a regime in the phase diagram spanned by the temperature and the coupling $\lambda_{\psi}^{\text{UV}}$ in which the chiral and the deconfinement phase transition are tightly linked. In this section, we would like to map this phase diagram onto a phase diagram spanned by the temperature and an IR observable of QCD, e. g. the chiral condensate $|\langle \bar{\psi}\psi \rangle|^{1/3}$ or the pion decay constant f_{π} .

In QCD we have only one input parameter, e. g. the strong coupling α_s at a (high) momentum scale or, equivalently, Λ_{QCD} . For vanishing current quark masses Λ_{QCD} determines all physical observables, such as the pion decay constant $f_{\pi} \sim \Lambda_{\text{QCD}}$ as well as the deconfinement and the chiral phase transition temperature, $T_d \sim \Lambda_{\text{QCD}}$ and $T_{\chi} \sim \Lambda_{\text{QCD}}$. Thus, real QCD in a phase diagram spanned by the temperature T/Λ_{QCD} and $f_{\pi}/\Lambda_{\text{QCD}}$ is a single point. In the present paper the scale Λ_{QCD} is fixed by the input for the background field $\langle A_0 \rangle$. In contradistinction to real QCD, however, an additional parameter is present in our study, namely $\lambda_{\psi}^{\text{UV}}$. In the following we shall consider this parameter as an asset which allows us to deform QCD. In our model, two-flavor QCD as defined by $f_{\pi} \approx 90 \text{ MeV}$ then corresponds to a specific choice for $\lambda_{\psi}^{\text{UV}}$ on a given RG trajectory. Thus, our deformed model effectively depends on two parameters, namely $\lambda_{\psi}^{\text{UV}}$ and Λ_{QCD} . In particular, the chiral phase transition temperature depends on two parameters in our study, namely $\lambda_{\psi}^{\text{UV}}$ and Λ_{QCD} , whereas the deconfinement phase transition temperature depends only on $\Lambda_{\text{QCD}} \sim T_d$. In the remainder of the paper we exploit the dependence of our model on $\lambda_{\psi}^{\text{UV}}$ in more detail to gain some insight into the relation of chiral and confining dynamics close to the finite-temperature phase boundary. Eventually, this leads to a prediction for a (T, f_{π}) phase diagram. We would like to add that deformations of QCD-like theories with an additional relevant param-

⁶ Strictly speaking we only have only a deconfinement crossover in the presence of light quarks.

ter, such as a four-fermion coupling, indeed play a prominent role in beyond-standard model applications, see e. g. Ref. [65].

For the computation of the (T, f_π) phase diagram we employ a (partially) bosonized version of our ansatz (3). Whereas the purely fermionic description is particularly convenient for analytic studies, the partially bosonized ansatz allows us to resolve momentum dependences of fermionic self-interactions in a simple manner and therefore permits a study of the formation of the chiral condensate and the mass spectrum of mesons. To obtain the partially bosonized formulation of our ansatz (3) we perform a Hubbard-Stratonovich transformation of the underlying path-integral [66, 67]. This introduces auxiliary fields $\bar{\Phi}^T = (\sigma, \vec{\pi})$ into the theory which mediate the interaction between the quarks. Here, we assume that the bosons are composites of fermions and do not carry an internal charge, e. g. color or flavor: $\sigma \sim (\bar{\psi}\psi)$ and $\vec{\pi} \sim (\bar{\psi}\vec{\tau}\gamma_5\psi)$. The components of $\bar{\Phi}$ are labeled according to the role that the corresponding fields are playing in the spontaneously broken regime. The effective action of the partially bosonized theory then reads⁷

$$\begin{aligned} \Gamma_k[\bar{\psi}, \psi, \bar{\Phi}, \langle A_0 \rangle] = & \int d^4x \left\{ Z_\psi \bar{\psi} (i\not{\partial} + \bar{g}\gamma_0 \langle A_0 \rangle) \psi \right. \\ & + \frac{1}{2} Z_\Phi (\partial_\mu \bar{\Phi})^2 + i\bar{h} \bar{\psi} (\sigma + i\vec{\tau} \cdot \vec{\pi} \gamma_5) \psi \\ & \left. + \frac{1}{2} \bar{m}^2 \bar{\Phi}^2 + \frac{1}{8} \bar{\lambda}_\Phi \bar{\Phi}^4 \right\}, \end{aligned} \quad (23)$$

with a Yukawa coupling $\bar{h} \in \mathbb{R}$ and the boundary conditions

$$\lim_{k \rightarrow \Lambda} Z_\Phi = 0, \quad (24)$$

$$\lim_{k \rightarrow \Lambda} Z_\psi = 1, \quad (25)$$

$$\lim_{k \rightarrow \Lambda} \bar{\lambda}_\Phi = 0. \quad (26)$$

These boundary conditions together with the identity

$$\bar{\lambda}_\psi = \frac{\bar{h}^2}{\bar{m}^2} \quad (27)$$

allow us to map the ansatz (23) onto the model (3) at the initial UV scale Λ . In particular, we are now able to relate the initial values λ_ψ^{UV} to physically meaningful IR observables, e. g. the pion decay constant and the chiral condensate.

The term $\sim \bar{\Phi}^4$ in the effective action (23) corresponds to an 8-fermion interaction term in the purely fermionic description, $\bar{\Phi} \sim \bar{\psi}\psi$. Due to the boundary condition (26) this term is generated dynamically and not adjusted by hand in our RG approach, see e. g. [15, 19, 37, 62, 63]. Thus, the value of the corresponding coupling at the initial RG scale Λ does not represent an additional parameter of the theory. In any case, this coupling only plays a prominent role in the deep IR regime where it accounts for the mass difference between the σ -meson and the pions.

A word of caution concerning the mapping of the partially bosonized and the purely fermionic description needs to be added here. The identity (27) suggests that we indeed have only one input parameter in the present study, namely the value of the ratio $\bar{h}_{\text{UV}}^2/\bar{m}_{\text{UV}}^2$ at the UV scale Λ . In $d = 4$ space-time dimensions, however, the Yukawa coupling \bar{h} is marginal. This suggests that the partially bosonized theory in $d = 4$ depends on two input parameters in contrast to $d = 3$, see Refs. [63, 68]. Nonetheless the critical scale k_{cr} only depends on the ratio $\bar{h}_{\text{UV}}^2/\bar{m}_{\text{UV}}^2$ in leading order in an expansion in powers of $1/N_c$ and receives only small corrections from the next-to-leading order, see below. On the other hand, the ratio of IR observables, such as the ratio of the σ mass and the constituent quark mass, depends on both parameters [68]. In the following we choose the ratio $\bar{h}_{\text{UV}}^2/\bar{m}_{\text{UV}}^2$ and the Yukawa coupling \bar{h}_{UV} as the independent input parameters at the UV scale Λ .

Let us now discuss the RG flow equations of the dimensionless renormalized couplings $m^2 = \bar{m}^2/(Z_\Phi k^2)$, $\lambda_\Phi = \bar{\lambda}_\Phi/Z_\Phi^2$ and the Yukawa coupling $h = \bar{h}/(Z_\Phi^{1/2} Z_\psi)$. Using the ansatz (23) together with the parametrization (6) of the fermion propagator we find

$$\begin{aligned} \partial_t m^2 = & (\eta_\Phi - 2)m^2 - \frac{3}{2\pi^2} l_1(\tau, m^2) \lambda_\Phi \\ & + \frac{4}{\pi^2} \sum_{l=1}^{N_c} l_1^{(\text{F})}(\tau, m_q^2, \nu_l |\phi|) h^2, \end{aligned} \quad (28)$$

$$\begin{aligned} \partial_t \lambda_\Phi = & 2\eta_\Phi \lambda_\Phi + \frac{3}{\pi^2} l_2(\tau, m^2) \lambda_\Phi^2 \\ & - \frac{8}{\pi^2} \sum_{l=1}^{N_c} l_2^{(\text{F})}(\tau, m_q^2, \nu_l |\phi|) h^4, \end{aligned} \quad (29)$$

$$\begin{aligned} \partial_t h^2 = & (\eta_\Phi + 2\eta_\psi) h^2 \\ & - \frac{2}{\pi^2} \frac{1}{N_c} \sum_{l=1}^{N_c} l_{1,1}^{(\text{FB})}(\tau, m_q^2, \nu_l |\phi|, m^2) h^4, \end{aligned} \quad (30)$$

where $\eta_\Phi = -\partial_t \ln Z_\Phi$ and $\eta_\psi = -\partial_t \ln Z_\psi$. The threshold functions are defined in App. A. Note that the quarks are massless in the symmetric regime, $m_q \equiv 0$.

At this point it is instructive to have a closer look at the mapping between the partially bosonized and the purely fermionic description. To this end, we consider the RG flow of the ratio h^2/m^2 which can be obtained straightforwardly from the flow equations (28) and (30).

⁷ At finite temperature the Poincare invariance of the theory is broken. Therefore the wave-function renormalizations longitudinal and transversal to the heat-bath obey a different RG running. We neglect this difference in the present work. This is justified since it has indeed been found in Ref. [63] that the difference is small at low temperatures and only yields mild corrections to, e. g., the thermal mass of the bosonic degrees of freedom for intermediate temperatures $T \gtrsim T_\chi$.

We obtain

$$\begin{aligned} \partial_t \left(\frac{h^2}{m^2} \right) &= (2+2\eta_\psi) \left(\frac{h^2}{m^2} \right) + \frac{3}{2\pi^2} l_1(\tau, m^2) \lambda_\Phi \left(\frac{h^2}{m^4} \right) \\ &\quad - \frac{4}{\pi^2} \sum_{l=1}^{N_c} l_1^{(F)}(\tau, m_q^2, \nu_l |\phi|) \left(\frac{h^2}{m^2} \right)^2 \\ &\quad - \frac{2}{\pi^2} \frac{1}{N_c} \sum_{l=1}^{N_c} l_{1,1}^{(FB)}(\tau, m_q^2, \nu_l |\phi|, m^2) \left(\frac{h^4}{m^2} \right). \end{aligned} \quad (31)$$

Using Eqs. (26) and (27) as well as

$$l_{1,1}^{(FB)}(\tau, m_q^2, \nu_l |\phi|, m^2) \xrightarrow{(m \gg 1)} \frac{1}{m^2} l_1^{(F)}(\tau, m_q^2, \nu_l |\phi|), \quad (32)$$

we recover the RG flow equation (7) of the four-fermion coupling λ_ψ . Thus, the partially bosonized and the purely fermionic description are indeed identical at the UV scale Λ . Note that the prefactor of the term $\sim h^2/m^2$ would turn out to be incorrect if we did not include the RG running of the Yukawa coupling. In other words, a standard local potential approximation does not incorporate all terms associated with a systematic expansion of the flow equations in powers of $1/N_c$. In Ref. [68] this observation is discussed in the context of the Gross-Neveu model.

From Eq. (31) we also deduce that the partially bosonized description allows us to go conveniently beyond the point-like approximation employed in the purely fermionic description discussed in Sect. II. To be more specific, we observe that the momentum dependence of the four-fermion vertex is effectively parametrized by the RG flow of the four-boson coupling λ_Φ , the Yukawa coupling h and the mass parameter m^2 . We stress that the purely fermionic point-like description and the partially bosonized description are no longer identical for scales $k < \Lambda$. From the flow equation of the ratio h^2/m^2 , however, it follows that the differences are quantitatively small in the symmetric regime since the renormalized mass of the mesons is large.

In the regime with broken chiral symmetry in the ground state the mass parameter m^2 assumes negative values. This behavior signals the existence of a finite vacuum expectation value of the field Φ . In this regime, it is therefore convenient to study the RG flow of the four-boson coupling λ_Φ and the vacuum expectation value $\langle \Phi \rangle \equiv \Phi_0$. The RG flow of the latter can be obtained from the following condition:

$$\frac{d}{dt} \left[\frac{\partial}{\partial \Phi^2} \left(\frac{1}{2} \bar{m}^2 \bar{\Phi}^2 + \frac{1}{8} \bar{\lambda}_\Phi \bar{\Phi}^4 \right) \right]_{\bar{\Phi}_0} \stackrel{!}{=} 0. \quad (33)$$

The flow equations for Φ_0 and λ_Φ are then given by

$$\begin{aligned} \partial_t \Phi_0^2 &= -(\eta_\Phi + 2) \Phi_0^2 + \frac{3}{2\pi^2} l_1(\tau, m_\sigma^2) + \frac{3}{2\pi^2} l_1(\tau, m_\pi^2) \\ &\quad - \frac{8}{\pi^2} \sum_{l=1}^{N_c} l_1^{(F)}(\tau, m_q^2, \nu_l |\phi|) \frac{h^2}{\lambda_\Phi}, \end{aligned} \quad (34)$$

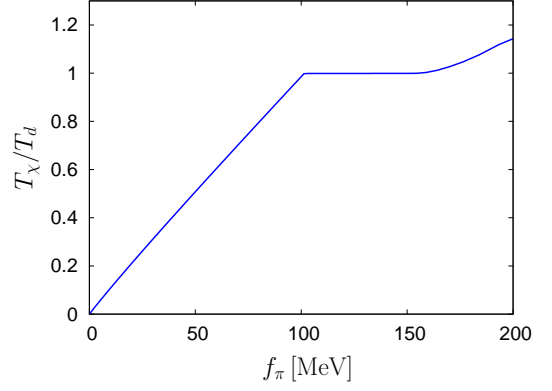


Figure 5: Phase diagram for two massless quark flavors and $N_c = 3$ in the plane spanned by the rescaled temperature T_χ/T_d and the value of the pion decay constant f_π at $T = 0$. The line depicts our result for the ratio T_χ/T_d of the chiral and the deconfinement phase transition temperature.

$$\begin{aligned} \partial_t \lambda_\Phi &= 2\eta_\Phi \lambda_\Phi + \frac{9}{4\pi^2} l_2(\tau, m_\sigma^2) \lambda_\Phi^2 + \frac{3}{4\pi^2} l_2(\tau, m_\pi^2) \lambda_\Phi^2 \\ &\quad - \frac{8}{\pi^2} \sum_{l=1}^{N_c} l_2^{(F)}(\tau, m_q^2, \nu_l |\phi|) h^4, \end{aligned} \quad (35)$$

where $m_\sigma^2 = \lambda_\Phi \Phi_0^2$, $m_\pi^2 = 0$ and $m_q^2 = h^2 \Phi_0^2$ is the constituent quark mass. Note that we identify $Z_\Phi^{-1/2} \bar{\Phi}_0$ with the pion decay constant f_π . For simplicity, we neglect the running of the Yukawa coupling in the regime with a broken chiral symmetry of the ground-state. In fact, 1PI diagrams with at least one internal quark line are parametrically suppressed in this regime since the quarks acquire a (large) mass. Therefore the RG flow of the theory in the spontaneously broken regime is mainly governed by 1PI diagrams with internal pion lines only. However, the latter class of diagrams does not directly contribute to the RG flow of the Yukawa coupling⁸.

In the present study we also neglect the running of the bosonic and fermionic wave-function renormalizations. Thus, we consider $Z_\Phi \equiv 1$ and $Z_\psi \equiv 1$. In studies with vanishing gluonic background field [15, 19, 62] it has indeed been found that the associated anomalous dimensions η_Φ and η_ψ are small over a wide range of scales. Nonetheless using $Z_\Phi \equiv 1$ means that we violate the initial condition $m^2 \gg 1$ for the renormalized mass at the UV scale Λ . The latter condition is equivalent to the condition (24). Therefore our study of the partially bosonized theory necessarily relies on two parameters instead of one, e. g. the initial values for h^2 and h^2/m^2 , which we expect to be anyway the case, see discussion

⁸ In the symmetric regime we have only taken into account the contributions to the running of the Yukawa coupling h which are required to map the flow of the ratio h^2/m^2 onto the RG flow of the four-fermion coupling λ_ψ at the UV scale Λ .

above. Employing $Z_\Phi \equiv 1$ then seems to be a reasonable approximation for a first explorative study of the locking mechanism discussed in Sect. II. In contrast to the flow of Z_Φ , the RG flow of Z_ψ is solely driven by 1PI diagrams with at least one internal boson and one internal fermion line. Since the mesons are heavy in the symmetric regime and the fermions are heavy in the regime with broken chiral symmetry in the ground state, it is justified to consider $Z_\psi \equiv 1$ for our purposes. For a more quantitative study including a determination of critical exponents, however, the running of Z_ψ , Z_Φ and the Yukawa coupling needs to be taken into account in both regimes since very close to the phase transition both the mesons and the quarks are approximately massless. The corresponding RG flow equations can be derived along the lines of, e. g., Refs. [15, 19, 62].

Using the partially bosonized theory we now estimate the size of the locking window for the chiral phase transition in terms of the pion decay constant f_π . The latter is directly related to the chiral condensate $|\langle\bar{\psi}\psi\rangle|^{1/3}$ via the Gell-Mann-Oakes-Renner relation. In Fig. 5 we present our result for the phase boundary for two massless quark flavors and $N_c = 3$ in the plane spanned by the temperature and the value of the pion decay constant at $T = 0$. This phase diagram corresponds to the phase diagram discussed in Sect. II. To obtain Fig. 5 we have set $\Lambda = 1$ GeV and used $h_{UV} = 3$ as initial condition at $k = \Lambda$. Different initial values for $\lambda_\psi^{UV} = h_{UV}^2/m_{UV}^2$ then translate into different values for f_π . In addition, we have employed the results for $\langle A_0 \rangle$ as obtained from a RG study of $SU(3)$ Yang-Mills theory [33, 39] which is in very good agreement with lattice QCD results. We neglect the back-reaction of the matter sector on $\langle A_0 \rangle$ and use only the Yang-Mills approximation for $\langle A_0 \rangle$ here to explore the impact of the discussed locking mechanism on the finite-temperature phase structure.

In Fig. 5 we notice that the chiral phase transition temperature tends to zero for $f_\pi \rightarrow 0$ and that T_χ is a monotonic function for small values of f_π , $T_\chi \sim f_\pi$. For $0 \leq f_\pi \lesssim 100$ MeV and $f_\pi \gtrsim 150$ MeV we observe a splitting of the phase boundary. Interestingly, we have $T_\chi > T_d$ for $f_\pi \gtrsim 150$ MeV and $T_\chi < T_d$ for $f_\pi \lesssim 100$ MeV. As a non-trivial result we find that the chiral phase transition is locked to the deconfinement phase transition for $100 \text{ MeV} \lesssim f_\pi \lesssim 150 \text{ MeV}$.⁹ This observation confirms our results from the study of the fixed-point structure in the purely fermionic description. Moreover, we find that the physically relevant range of values of the pion decay constant lies right below the locking window. The near coincidence of the two phase transition temperatures for $f_\pi \sim 90$ MeV has also been

found in an RG study including the back-reaction of the quark fluctuations on the order-parameter potential [37]. Recall that for $f_\pi \lesssim 150$ MeV the chiral phase transition temperature is shifted to larger values compared to studies with $\langle A_0 \rangle \equiv 0$ since the thermal excitation of quarks is suppressed by the confining dynamics in the gauge sector, see Eq. (15). Loosely speaking, we observe a competition between the confining dynamics and the thermal excitation of the system. While an increase of the temperature tends to restore chiral symmetry, the confining dynamics in the gauge sector favors a ground state with broken chiral symmetry.

For $f_\pi \gtrsim 150$ MeV, which corresponds to constituent quark masses $m_q \gtrsim 450$ MeV, we find a second-order chiral phase transition for vanishing current quark masses. Moreover, our result for T_χ as a function of f_π does not depend on the presence of the gluonic background field $\langle A_0 \rangle$ any more. In this regime, we expect that our results are least affected by our approximation of neglecting the back-reaction of the matter sector on the deconfinement order parameter. Here, the dynamics in the gauge sector and the matter sector are expected to be effectively decoupled. Nonetheless the difference between T_χ and T_d might be smaller in a full QCD study.

For $f_\pi \lesssim 150$ MeV a window may open up in which the chiral phase transition is of first order. This is due to the significant shift of the chiral phase transition temperature to larger values in this regime compared to the case without a gluonic background field. Provided the deconfinement order parameter rises quickly above the (deconfinement) phase transition [33, 34, 39, 69], strong thermal excitations may induce a chiral transition of first order. In our present study we indeed find a first-order chiral phase-transition for $100 \text{ MeV} \lesssim f_\pi \lesssim 150 \text{ MeV}$. However, we rush to add that this observation is a shortcoming of our approximations since we have employed the results for $\langle A_0 \rangle$ as obtained from a study of $SU(3)$ Yang-Mills theory but neglected the back-reaction of the matter sector on $\langle A_0 \rangle$. Thus, the first-order phase transition in the gauge sector induces a first-order chiral phase transition in this regime. Nevertheless a first-order chiral phase transition may occur in this regime even if we include the back-reaction of the matter sector on the confinement order parameter, provided the latter rises rapidly for $T \gtrsim T_d$. For example, this might be the case for physical pion masses. In this respect the present analysis provides a simple mechanism for a first-order chiral phase transition [70]. For $f_\pi \lesssim 100$ MeV we find again a second-order chiral phase transition for vanishing current quark masses.

We would like to remind the reader of the fact that we have only one parameter in QCD with massless current quarks and that four-fermion interactions are induced by fluctuations, e. g. two-gluon exchange; see Refs. [15–20] for a detailed discussion. In the present paper we have considered the initial value λ_ψ^{UV} of the four-fermion coupling as an additional parameter which allowed us to deform QCD and study some aspects of the relation of

⁹ Using $h_{UV} = 3.5$ as initial condition for the Yukawa coupling, we find that the value of the lower end of this window for f_π is lowered by approximately 10%. However, the size of this window is roughly independent of the considered initial conditions for the Yukawa coupling.

quark confinement and chiral symmetry breaking. In any case, we would like to stress that the relation of the fixed-point structure in the matter sector to the deconfinement order parameter is a universal statement which is *a priori* independent of the details of the actual scale fixing procedure. This interplay of the matter and the gauge sector suggests the existence of a window for the values of the physical observables in which the chiral and the deconfinement phase transition lie close to each other.

IV. CONCLUSIONS AND OUTLOOK

In the present paper we have analyzed the interplay of the deconfinement and the chiral phase transition. To this end, we have studied the fixed-point structure of four-fermion interactions in the presence of a finite temporal gluonic background field. The latter can be directly related to an order parameter for the deconfinement phase transition, namely $\text{tr}_F L[\langle A_0 \rangle] \geq \langle \text{tr}_F L[A_0] \rangle$. In a purely fermionic description the onset of chiral symmetry breaking is indicated by rapidly increasing four-fermion interactions. Restoration of chiral symmetry is then displayed by four-fermion couplings which approach a Gaussian fixed point in the IR. Thus, the question of chiral symmetry breaking in the IR can ultimately be linked to the fixed-point structure of the four-fermion couplings.

We have indeed found that the fixed-point structure of four-fermion interactions is directly related to the order parameter for confinement. In particular, we have analyzed the scalar-pseudoscalar interaction channel and have shown that its β function does not depend on the temperature in the limit $N_c \rightarrow \infty$, provided we are in the confined phase, i. e. $\text{tr}_F L[\langle A_0 \rangle] \rightarrow 0$. Loosely speaking, thermal excitations of the quarks are suppressed in the confined phase. Therefore the chiral phase transition is locked in and shifted to higher temperatures. Our findings confirm the results of a mean-field study by Meisinger and Ogilvie [3] in which it has been pointed out that the chiral order-parameter potential is independent of the temperature in the confined phase by employing the assumption $\text{tr}_F L[\langle A_0 \rangle] = \langle \text{tr}_F L[A_0] \rangle$. Our non-perturbative analysis of the fixed-point structure of the matter sector establishes this observation. However, we have not made use of the assumption $\text{tr}_F L[\langle A_0 \rangle] = \langle \text{tr}_F L[A_0] \rangle$. In fact, our study shows that the latter assumption is only justified in the limit $N_c \rightarrow \infty$. Moreover, we have studied how corrections to the large- N_c approximation affect the dynamics at the finite-temperature phase boundary. The locking mechanism discussed in Sect. II eventually allows us to determine a window for the values of the pion decay constant in which the chiral and the deconfinement phase transition lie close to each other. The size of this window depends on the number of colors N_c and is maximal in the limit $N_c \rightarrow \infty$.

For $N_c = 3$ and two massless quark flavors we have computed the phase diagram in the plane spanned by the

temperature and the pion decay constant. This phase diagram can be divided into three different regimes. For small values of f_π we find a regime with $T_d > T_\chi$. For $100 \text{ MeV} \lesssim f_\pi \lesssim 150 \text{ MeV}$ the deconfinement and the chiral phase transition lie close to each other. Finally, there is a third regime for $f_\pi \gtrsim 150 \text{ MeV}$ which is characterized by $T_\chi > T_d$. Here, the chiral condensate is large and therefore the matter and the gauge sector are effectively decoupled.

Of course, the present study can be improved in many ways. Currently we are including the contributions to the RG flow of the four-fermion coupling arising from 1PI diagrams with one- or two internal gluon lines [71]. This will eventually allow us to get rid of the parameter λ_ψ^{UV} so that we are left with a single parameter for the gauge and the matter sector, namely α_s at a given UV scale.

While a study of the QCD phase diagram in the (T, μ) plane is of great phenomenological importance, we think that a study of the phase diagram in the (T, f_π) plane (or equivalently in the $(T, |\langle \bar{\psi}\psi \rangle|^{1/3})$ plane) may provide us with important insights concerning the interplay of chiral and confining dynamics. In particular, such a study of the (T, f_π) phase diagram does not suffer from problems arising, e. g., from a complex-valued spectrum of the Dirac operator as it is the case at finite quark chemical potential μ . Therefore, an analysis of the (T, f_π) phase diagram may be also helpful to benchmark results from continuum approaches against those from lattice QCD simulations.

Acknowledgments

The authors are very grateful to H. Gies, B. Klein and J. M. Pawłowski for useful discussions and a critical reading of the manuscript. JB acknowledges support by the DFG research training group GRK 1523/1.

Appendix A: Threshold functions

In this appendix we summarize technical details concerning the derivation of the RG flow equations.

In the computation of the RG flow equations a regulator function needs to be specified which determines the regularization scheme [52]. In the present work we have employed an optimized spatial regulator function for the bosonic as well as for the fermionic degrees of freedom [72–76]. For the bosons, we choose

$$R_B(\vec{p}^2) = \vec{p}^2 \left(\frac{k^2}{\vec{p}^2} - 1 \right) \theta(k^2 - \vec{p}^2) \equiv \vec{p}^2 r_B \left(\frac{\vec{p}^2}{k^2} \right), \quad (\text{A1})$$

whereas we choose

$$R_\psi(\vec{p}) = \vec{p} \left(\sqrt{\frac{k^2}{\vec{p}^2}} - 1 \right) \theta(k^2 - \vec{p}^2) \equiv \vec{p} r_\psi \left(\frac{\vec{p}^2}{k^2} \right) \quad (\text{A2})$$

for the fermionic degrees of freedom. In the following we define the threshold functions relevant for the present work. These functions represent the 1PI diagrams contributing to the RG flow of the studied couplings. For a generalizations of the threshold functions to an arbitrary number of space-time dimensions we refer the reader to Ref. [19] where also the dependence of these functions on the anomalous dimensions is displayed. The latter is of no relevance for the present study.

In order to define the threshold functions, it is convenient to define dimensionless propagators for the bosons (B) and the fermions (ψ), respectively:

$$\tilde{G}_B(x_0, \omega) = \frac{1}{x_0 + x(1 + r_B) + \omega} \quad (\text{A3})$$

and

$$\tilde{G}_\psi(x_0, \omega) = \frac{1}{x_0 + x(1 + r_\psi)^2 + \omega}, \quad (\text{A4})$$

where $x = \vec{p}^2/k^2$.

First, we define the threshold functions which appear in the RG flow equations for the bosonic self-interactions. For the purely bosonic loops, we find

$$\begin{aligned} l_0(\tau, \omega) &= \frac{\tau}{2} \sum_{n=-\infty}^{\infty} \int_0^{\infty} dx x^{\frac{3}{2}} (\partial_t r_B) \tilde{G}_B(\tilde{\omega}_n^2, \omega) \\ &= \frac{2}{3} \frac{1}{\sqrt{1+\omega}} \left(\frac{1}{2} + \bar{n}_B(\tau, \omega) \right) \end{aligned} \quad (\text{A5})$$

where $\tau = T/k$ denotes the dimensionless temperature and $\tilde{\omega}_n = 2\pi n\tau$ denotes the dimensionless bosonic Matsubara frequencies. The function \bar{n}_B represents the Bose-Einstein distribution function:

$$\bar{n}_B(\tau, \omega) = \frac{1}{e^{\sqrt{1+\omega}/\tau} - 1}. \quad (\text{A6})$$

Bosonic threshold functions of order n are then derived from Eq. (A5) by taking derivatives with respect to the mass parameter ω :

$$\frac{\partial}{\partial \omega} l_n(\tau, \omega) = -(n + \delta_{n,0}) l_{n+1}(\tau, \omega). \quad (\text{A7})$$

For the purely fermionic loops contributing to the flow equations of the bosonic self-interactions but also to the RG flow of the four-fermion coupling, we find

$$\begin{aligned} l_0^{(F)}(\tau, \omega, \mu) &= \tau \sum_{n=-\infty}^{\infty} \int_0^{\infty} dx x^{\frac{3}{2}} (\partial_t r_\psi) (1 + r_\psi) \times \\ &\quad \times \tilde{G}_\psi((\tilde{\nu}_n + 2\pi\tau\mu)^2, \omega) \\ &= \frac{1}{3} \frac{1}{\sqrt{1+\omega}} (1 - \bar{n}_\psi(\tau, i\mu, \omega) - \bar{n}_\psi(\tau, -i\mu, \omega)). \end{aligned} \quad (\text{A8})$$

Here, we have introduced the dimensionless fermionic Matsubara frequencies $\tilde{\nu}_n = (2n + 1)\pi\tau$. The function \bar{n}_ψ represents the Fermi-Dirac distribution function:

$$\bar{n}_\psi(\tau, \mu, \omega) = \frac{1}{e^{(\sqrt{1+\omega}/\tau) + 2\pi\mu} + 1}. \quad (\text{A9})$$

Higher-order fermionic threshold functions can again be found by taking derivatives with respect to the mass parameter ω :

$$\frac{\partial}{\partial \omega} l_n^{(F)}(\tau, \omega, \mu) = -(n + \delta_{n,0}) l_{n+1}^{(F)}(\tau, \omega, \mu). \quad (\text{A10})$$

To prove Eq. (20) it is convenient to perform the sum over Matsubara frequencies. The threshold function $l_1^{(F)}$ can then be written as follows

$$\begin{aligned} l_1^{(F)}(\tau, 0, \mu) &= \int_0^{\infty} dx x^{\frac{3}{2}} (\partial_t r_\psi) (1 + r_\psi) \left\{ \frac{1}{4[f(x)]^{\frac{3}{2}}} \right. \\ &\quad - \frac{1}{2\tau[f(x)]^{3/2}[g(x, \mu)]^2} \left[2\tau e^{\frac{2\sqrt{f(x)}}{\tau}} [\cos(2\pi\mu)]^2 \right. \\ &\quad \left. + e^{\frac{\sqrt{f(x)}}{\tau}} \left(\sqrt{f(x)} \left(e^{\frac{2\sqrt{f(x)}}{\tau}} + 1 \right) \right. \right. \\ &\quad \left. \left. + \tau \left(e^{\frac{2\sqrt{f(x)}}{\tau}} + 3 \right) \right) \cos(2\pi\mu) + \tau e^{\frac{2\sqrt{f(x)}}{\tau}} \right. \\ &\quad \left. \left. + 2\sqrt{f(x)} e^{\frac{2\sqrt{f(x)}}{\tau}} + \tau \right] \right\}, \end{aligned} \quad (\text{A11})$$

where $f(x) = x(1 + r_\psi)^2$ and

$$g(x, \mu) = 2 e^{-\frac{\sqrt{f(x)}}{\tau}} \cos(2\pi\mu) + e^{-\frac{2\sqrt{f(x)}}{\tau}} + 1. \quad (\text{A12})$$

The first term in the curly bracket on the right-hand side of Eq. (A11) is the zero-temperature contribution which is strictly positive. The second term (square bracket) corresponds to the finite-temperature corrections and is strictly negative, provided that $\cos(2\pi\mu) > 0$. For regulator functions with $(\partial_t r_\psi) \geq 0$ we then find that the finite-temperature corrections yield a negative contribution to $l_1^{(F)}$. In the RG flow equation of the four-fermion coupling we sum over the eigenvalues $\mu = \nu_l |\phi|$. Since

$$\sum_{l=1}^{N_c} \cos(2\pi\nu_l |\phi|) \geq 0 \quad (\text{A13})$$

for $N_c = 2$ and $N_c = 3$, we have proven Eq. (20).

Finally we give the definition of the threshold function which appears in the RG flow equations of the Yukawa coupling. We have

$$\begin{aligned} l_{1,1}^{(FB)}(\tau, \omega_\psi, \mu, \omega_B) &= -\frac{\tau}{2} \sum_{n=-\infty}^{\infty} \int_0^{\infty} dx x^{\frac{1}{2}} \tilde{\partial}_t \left\{ \tilde{G}_\psi((\tilde{\nu}_n + 2\pi\tau\mu)^2, \omega_\psi) \times \right. \\ &\quad \left. \times \tilde{G}_B(\tilde{\nu}_n^2, \omega_B) \right\}. \end{aligned} \quad (\text{A14})$$

To evaluate the integral over x (spatial momenta), we have to take derivatives with respect to the regulator function. For the regulator functions (A1) and (A2) these derivatives are given by

$$\tilde{\partial}_t \Big|_\psi = \frac{1}{x^{1/2}} \theta(1-x) \frac{\partial}{\partial r_\psi}, \quad (\text{A15})$$

$$\tilde{\partial}_t \Big|_B = \frac{2}{x} \theta(1-x) \frac{\partial}{\partial r_B}, \quad (\text{A16})$$

where the first and the second line defines how the formal derivative $\tilde{\partial}_t$ acts on the fermion propagator and the

boson propagator, respectively.

-
- [1] P. Braun-Munzinger, K. Redlich, and J. Stachel (2003), nucl-th/0304013.
 - [2] L. McLerran and R. D. Pisarski, Nucl. Phys. **A796**, 83 (2007), 0706.2191.
 - [3] P. N. Meisinger and M. C. Ogilvie, Phys. Lett. **B379**, 163 (1996), hep-lat/9512011.
 - [4] R. D. Pisarski, Phys. Rev. **D62**, 111501 (2000), hep-ph/0006205.
 - [5] A. Mocsy, F. Sannino, and K. Tuominen, Phys. Rev. Lett. **92**, 182302 (2004), hep-ph/0308135.
 - [6] K. Fukushima, Phys. Lett. **B591**, 277 (2004), hep-ph/0310121.
 - [7] E. Megias, E. Ruiz Arriola, and L. L. Salcedo, Phys. Rev. **D74**, 065005 (2006), hep-ph/0412308.
 - [8] C. Ratti, M. A. Thaler, and W. Weise, Phys. Rev. **D73**, 014019 (2006), hep-ph/0506234.
 - [9] C. Sasaki, B. Friman, and K. Redlich, Phys. Rev. **D75**, 074013 (2007), hep-ph/0611147.
 - [10] B.-J. Schaefer, J. M. Pawłowski, and J. Wambach, Phys. Rev. **D76**, 074023 (2007), 0704.3234.
 - [11] A. J. Mizher, M. N. Chernodub, and E. S. Fraga, Phys. Rev. **D82**, 105016 (2010), 1004.2712.
 - [12] V. Skokov, B. Stokic, B. Friman, and K. Redlich, Phys. Rev. **C82**, 015206 (2010), 1004.2665.
 - [13] T. K. Herbst, J. M. Pawłowski, and B.-J. Schaefer, Phys. Lett. **B696**, 58 (2011), 1008.0081.
 - [14] V. Skokov, B. Friman, and K. Redlich (2010), 1008.4570.
 - [15] H. Gies and C. Wetterich, Phys. Rev. **D69**, 025001 (2004), hep-th/0209183.
 - [16] H. Gies and J. Jaeckel, Eur. Phys. J. **C46**, 433 (2006), hep-ph/0507171.
 - [17] J. Braun and H. Gies, Phys. Lett. **B645**, 53 (2007), hep-ph/0512085.
 - [18] J. Braun and H. Gies, JHEP **06**, 024 (2006), hep-ph/0602226.
 - [19] J. Braun, Eur. Phys. J. **C64**, 459 (2009), 0810.1727.
 - [20] J. Braun and H. Gies, JHEP **05**, 060 (2010), 0912.4168.
 - [21] J. Braun, C. S. Fischer, and H. Gies (2010), 1012.4279.
 - [22] M. Cheng et al., Phys. Rev. **D74**, 054507 (2006), hep-lat/0608013.
 - [23] Y. Aoki, Z. Fodor, S. D. Katz, and K. K. Szabo, Phys. Lett. **B643**, 46 (2006), hep-lat/0609068.
 - [24] Y. Aoki, G. Endrodi, Z. Fodor, S. D. Katz, and K. K. Szabo, Nature **443**, 675 (2006), hep-lat/0611014.
 - [25] Y. Aoki et al., JHEP **06**, 088 (2009), 0903.4155.
 - [26] M. Panero, Phys. Rev. Lett. **103**, 232001 (2009), 0907.3719.
 - [27] M. Cheng et al., Phys. Rev. **D81**, 054504 (2010), 0911.2215.
 - [28] S. Datta and S. Gupta, Phys. Rev. **D82**, 114505 (2010), 1006.0938.
 - [29] S. Borsanyi et al. (2010), 1011.4230.
 - [30] A. Bazavov and P. Petreczky, PoS **LATTICE2010**, 169 (2010), 1012.1257.
 - [31] K. Kanaya (2010), 1012.4235.
 - [32] V. G. Bornyakov et al. (2011), 1102.4461.
 - [33] J. Braun, H. Gies, and J. M. Pawłowski, Phys. Lett. **B684**, 262 (2010), 0708.2413.
 - [34] F. Marhauser and J. M. Pawłowski (2008), 0812.1144.
 - [35] C. S. Fischer, Phys. Rev. Lett. **103**, 052003 (2009), 0904.2700.
 - [36] C. S. Fischer and J. A. Mueller, Phys. Rev. **D80**, 074029 (2009), 0908.0007.
 - [37] J. Braun, L. M. Haas, F. Marhauser, and J. M. Pawłowski, Phys. Rev. Lett. **106**, 022002 (2011), 0908.0008.
 - [38] C. S. Fischer, A. Maas, and J. A. Muller, Eur. Phys. J. **C68**, 165 (2010), 1003.1960.
 - [39] J. Braun, A. Eichhorn, H. Gies, and J. M. Pawłowski, Eur. Phys. J. **C70**, 689 (2010), 1007.2619.
 - [40] J. M. Pawłowski (2010), 1012.5075.
 - [41] B.-J. Schaefer, M. Wagner, and J. Wambach, Phys. Rev. **D81**, 074013 (2010), 0910.5628.
 - [42] C. Gatttringer, Phys. Rev. Lett. **97**, 032003 (2006), hep-lat/0605018.
 - [43] F. Synatschke, A. Wipf, and C. Wozar, Phys. Rev. **D75**, 114003 (2007), hep-lat/0703018.
 - [44] E. Bilgici, F. Bruckmann, C. Gatttringer, and C. Hagen, Phys. Rev. **D77**, 094007 (2008), 0801.4051.
 - [45] K. Kashiwa, M. Matsuzaki, H. Kouno, Y. Sakai, and M. Yahiro, Phys. Rev. **D79**, 076008 (2009), 0812.4747.
 - [46] Y. Sakai, K. Kashiwa, H. Kouno, and M. Yahiro, Phys. Rev. **D77**, 051901 (2008), 0801.0034.
 - [47] E. Bilgici et al., Few Body Syst. **47**, 125 (2010), 0906.3957.
 - [48] B. Zhang, F. Bruckmann, C. Gatttringer, Z. Fodor, and K. K. Szabo (2010), 1012.2314.
 - [49] T. K. Mukherjee, H. Chen, and M. Huang, Phys. Rev. **D82**, 034015 (2010), 1005.2482.
 - [50] R. Gatto and M. Ruggieri, Phys. Rev. **D82**, 054027 (2010), 1007.0790.
 - [51] K.-I. Kondo, Phys. Rev. **D82**, 065024 (2010), 1005.0314.
 - [52] C. Wetterich, Phys. Lett. **B301**, 90 (1993).
 - [53] D. F. Litim and J. M. Pawłowski (1998), hep-th/9901063.
 - [54] C. Bagnuls and C. Bervillier, Phys. Rept. **348**, 91 (2001), hep-th/0002034.
 - [55] J. Berges, N. Tetradis, and C. Wetterich, Phys. Rept. **363**, 223 (2002), hep-ph/0005122.
 - [56] J. Polonyi, Central Eur. J. Phys. **1**, 1 (2003), hep-th/0110026.
 - [57] B. Delamotte, D. Mouhanna, and M. Tissier, Phys. Rev. **B69**, 134413 (2004), cond-mat/0309101.
 - [58] J. M. Pawłowski, Annals Phys. **322**, 2831 (2007), hep-th/0512261.
 - [59] H. Gies (2006), hep-ph/0611146.
 - [60] B. Delamotte (2007), cond-mat/0702365.
 - [61] O. J. Rosten (2010), 1003.1366.
 - [62] J. Berges, D. U. Jungnickel, and C. Wetterich, Phys. Rev. **D59**, 034010 (1999), hep-ph/9705474.
 - [63] J. Braun, Phys. Rev. **D81**, 016008 (2010), 0908.1543.
 - [64] H. Gies, J. Jaeckel, and C. Wetterich, Phys. Rev. **D69**, 105008 (2004), hep-ph/0312034.
 - [65] H. S. Fukano and F. Sannino, Phys. Rev. **D82**, 035021 (2010), 1005.3340.

- [66] J. Hubbard, Phys. Rev. Lett. **3**, 77 (1959).
- [67] R. Stratonovich, Dokl. Akad. Nauk. **115**, 1097 (1957).
- [68] J. Braun, H. Gies, and D. D. Scherer (2010), 1011.1456.
- [69] A. Dumitru, Y. Guo, Y. Hidaka, C. P. K. Altes, and R. D. Pisarski (2010), 1011.3820.
- [70] M. D’Elia, A. Di Giacomo, and C. Pica, Phys. Rev. **D72**, 114510 (2005), hep-lat/0503030.
- [71] J. Braun and A. Janot, (work in progress).
- [72] D. F. Litim, Phys. Lett. **B486**, 92 (2000), hep-th/0005245.
- [73] D. F. Litim, Int. J. Mod. Phys. **A16**, 2081 (2001), hep-th/0104221.
- [74] D. F. Litim, Phys. Rev. **D64**, 105007 (2001), hep-th/0103195.
- [75] D. F. Litim and J. M. Pawłowski, JHEP **11**, 026 (2006), hep-th/0609122.
- [76] J.-P. Blaizot, A. Ipp, R. Mendez-Galain, and N. Wschebor, Nucl. Phys. **A784**, 376 (2007), hep-ph/0610004.